SEISMIC FRAGILITY ANALYSIS OF CASE STUDY FAILURE OF SHOWA BRIDGE DURING 1964 NIIGATA EARTHQUAKE

Partha Bhowmik[1], Swagata DebRoy[2] and Rajib Saha[3]

[1,2,3] National Institute of Technology Agartala, Dept. of Civil Engineering, Jirania, Tripura (W)
e-mail: parthabhowmil14@gmail.com,swagatadevroy@gmail.com,rajib.iitbbsr@gmail.com

ABSTRACT: Seismic design of pile foundation has gained special attention in last few decades after experiencing significant failures due to liquefaction during moderate to severe earthquakes. Seismic soil-pile foundation-structure interaction (SSPSI) was considered as an important phenomenon to explain the pile failure mechanism. In this context, present study attempts to assess the vulnerability of case study of Showa bridge pile foundation embedded in liquefiable susceptible ground considering SSPSI using OPENSeesPL. Both soil and structural nonlinearity considered in this study. Fragility analysis is performed using Monte-Carlo simulation (MCS) and multiple strip analysis (MSA) technique to calculate the probability of failure. First, the developed numerical model offers a well agreement with the observed response of case study structure. Probabilistic results indicate that maximum bending moment and displacement in pile are found to be higher in case of inertial interaction which may be due to $P\text{-}\Delta$ effect. Fragility result infers significant vulnerability of pile foundation during liquefaction attributing serviceability, collapse and curvature ductility limit states criteria. While, curvature ductility demand criteria gives higher vulnerability concern for pile foundation in liquefied deposit and may be considered as governing seismic design criteria.

KEYWORDS: Fragility curves, OPENSeeSPL, Pile foundation, Showa bridge, SSPSI.

1   INTRODUCTION
Failure of pile foundation evidenced during several past earthquakes has drawn global attention to the earthquake geotechnical engineers for sustainable seismic design. The failure is primarily observed in soft clay or loose liquefiable deposits as referred in several case studies [1, 23, 29]. Seismic soil–pile foundation-superstructure interaction (SSPSI) was reported as the key phenomenon which may help to understand the failure mechanism of pile foundation [18, 28, 7]. Both effect of inertial and kinematic SSPSI interaction

on response of pile supported structure was critically investigated in several studies [30, 7]. The influence of both the interactions was reported to be important in seismic design. On the other hand, past studies also reported different soil structure interaction (SSI) modelling techniques which could reasonably predict the SSI response of structural systems [22, 36-38, 18, 31,28]. It was found that beams on nonlinear Winkler foundation (BNWF) model was well accepted due to its computational efficiency [e.g. 28, 2, 21]. However, the continuum based SSI model having nonlinear material characteristics may offer accurate prediction of response [32-35]. In this context, present study attempts to assess the post vulnerability analysis of a case study pile supported bridge structure (Showa bridge in Japan) which was failed during 1964 Niigata earthquake and remained an iconic example for the earthquake scientist and engineering community. Different hypothesis about failure mechanism of Showa bridge pile foundation have emerged. Bhattacharya *et al*. 2008 [3] primarily presented bending-buckling theory to define the failure mechanism of pile. Further, another study by the same group [2] has concluded that bending-buckling theory sole cannot explain the failure mechanism of pile of Showa Bridge and suggested resonating response of the whole structure can be the governing factor to expedite bending-bucking interaction which led to the failure of pile before commencement of lateral spreading. On the other hand, many researchers claimed that bridge failure has occurred only because of significant bending moment developed at pile head due to lateral spreading caused during liquefaction occurrence [5, 16, 4, 7].

From this viewpoint, it has been realized that vulnerability assessment of pile foundation, mainly in liquefiable deposit incorporating both inertial and kinematic interaction is essential. Zentner *et al*. (2016) [10] discussed different methods for fragility analysis to assess the seismic vulnerability of structures along with their advantages and disadvantages. This study further indicated that multiple strips analysis (MSA) is most reliable and simplified method for fragility analysis. On the other hand, some studies reported that ground motion characteristics have significant effect on seismic fragility analysis of structures [8,9]. It is also presented in some studies that variation in different parameters of ground motion, such as, frequency content, peak ground acceleration (PGA), peak ground velocity (PGV), spectral acceleration, duration of motion, moment magnitude and focal depth etc. are considered in vulnerability analysis [17]. In addition, several studies were performed to calculate the vulnerability of pile supported structure [20, 24, 26]. However, vulnerability analysis of pile foundation in liquefiable deposit is found to be limited. Hence, present study is an effort to assess the vulnerability of pile foundation embedded in liquefaction susceptible layer by performing probabilistic nonlinear dynamic analysis on a 3D FEM model using OPENSeesPL (V-2.7.2 2018) [42]. The case study of Showa bridge pile foundation is used in present analysis. Monte Carlo Simulation (MCS) is used for probabilistic analysis. Fragility analysis is

performed by incorporating randomly generated ground motions based on 'failure' and 'success' information gathered from multiple strip analysis and maximum likelihood estimation method. Both collapse and serviceability limit state criteria are used to represent the fragility curves. Furthermore, probability of failure (POF) with respect to ductility demand of pile is also calculated herein. Finally, the outcome of present study will help to provide significant design inputs for design of pile foundation in liquefiable soil.

2   MODELING OF SOIL-PILE FOUNDATION SYSTEM
2.1   Case study structural details
Details of Showa Bridge are taken from [2]. The bridge consisted of 12 composite girders. The total length of bridge was about 307 m. The main span was of about 28 m and side span of about 15 m length. A single bridge pier was composed of 9 tubular steel piles with 0.609 m outer diameter. The wall thickness of piles varied from 9 mm at the bottom 13m of pile and 16 mm at the upper 12m of pile. The cross sectional view of pile foundation system is shown in Figure 1. The 25 m long pile passes through a four-phase system of air, water, liquefied soil, and non-liquefied soil surrounding it. The first 10m soil is medium to coarse sand ($N{\leq}10$) and second 6.0 m is dense sand ($N{\leq}30$). Each pile group is designed to support gravity load of 6531.20 kN. The case study structure is modeled using 3D finite element OPENSeesPL software (V-2.7.2, 2018) and steps of modeling are presented in next subsection. Table 1 presents the detailed parameters of pile and soil.

2.2   Pile modeling
$1{\times}3$ pile group is modelled in OPENSeesPL [42] out of total nine piles in the present study. All parameters related to geometric and material properties of pile are kept same as [2]. Total dead and live load acting on each pile head is calculated as 800 kN. Accordingly, axial load is calculated for $1{\times}3$ pile group which is further used in subsequent analysis. The piles are modelled using displacement controlled beam column element having 8 numbers of slices. Bi-linear elasto-plastic material is assigned for pile element. The tip of pile is fixed with the assumption that pile will undergo zero vertical settlement. Four cases of axial loading condition i.e. 0%, 33%, 67%, and 100% of the total vertical load on the pile group are considered herein for simulating both kinematic and inertial interaction of the pile-soil system embedded in liquefaction susceptible ground. Figure 3 presents schematic idealization of both the interaction cases analysed in present study.
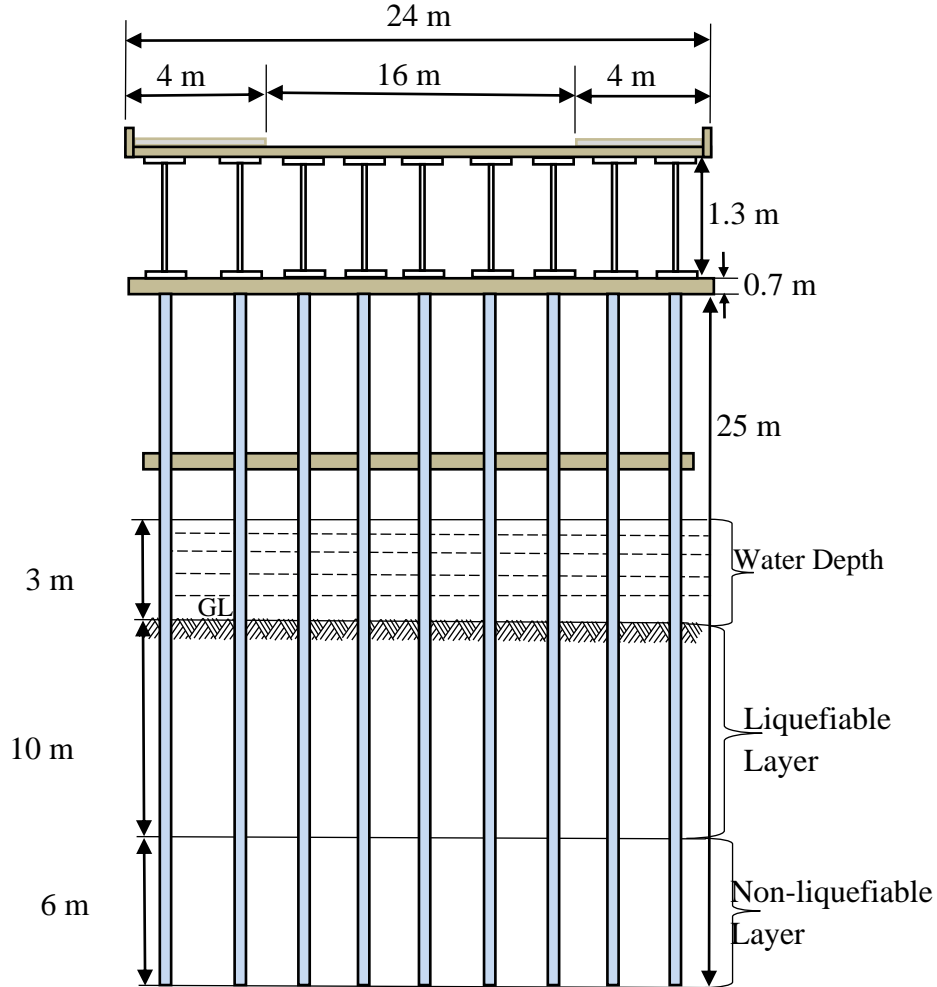
Figure 1. Cross sectional profile of Showa bridge

2.3 Modeling of soil domain

 The soil layer is idealized as top liquefiable layer up to 10m from ground
surface followed by another non-liquefiable layer having thickness of 6m as
shown in Figure 1. The dimension of soil domain is considered as 20 m long, 11
m wide and 10 m thick. Soil domain is discretised using three-dimensional 8
nodded brick element having three degrees of freedom (DOF) at each node.
Total numbers of nodes and brick elements are 105 and 48 respectively.
"*PressureDependMultiYield*" command from material library of OPENSeesPL
[42] is selected for soil modeling. This command creates an elastic-plastic
material to simulate response characteristics like dilatancy, cyclic mobility in
pressure sensitive soil material such as sand. However, the liquefaction

parameters are selected based on model suggested by [39]. The total number of yield surfaces of Drucker-Prager type is considered as 20. The lateral boundary is assigned as periodic boundary whereas the bottom layer below pile is assumed as fixed. The properties of both the stratum are presented in Table 1.

Table 1. Properties of pile and soil used in this study

Pile Parameters	Values	Soil Parameters	Liquefiable Layer (10m)	Non-Liquefiable layer (6m)
Outer diameter (D_o) (m)	0.609	Consistency of sand	Medium to loose	Dense
Internal diameter (D_i) (m)	0.591	N value	<10	>30
Pile Length (L) (m)	25	Saturated mass density (ρ_{sat}) (Mg/m^3)	1.7	2.1
Spacing to outer diameter ratio	2.2	Shear Modulus (G) (kPa)	55000	130000
Young's Modulus (E_s) (GPa)	210	Relative Density (ρ_s)	40%	>75%
Section Modulus (Z) (m^3)	0.0015	Friction Angle (ϕ)	29°	40°
Flexural strength of pile (MPa)	490			
Ultimate moment capacity of pile (M_u) (kN-m)	1286			
Plastic Moment capacity of pile (M_p) (kN-m)	2415			
Flexural Rigidity (kN-m^2)	160061.92			
Shear Rigidity (kN)	9063516			
Torsional Rigidity (kN- m^2)	1133228			
Axial Rigidity (kN)	23562000			

2.4 Modeling of soil-pile interface

The 3D brick element representing soil mass are connected to 1D pile element by rigid links through zero length element and equal translation constraint using *equalDOF* command. Figure 4 presents the schematic diagram of soil-pile interface modelling. The zero Length element connects the rigid link axially to adjacent soil node. 5% damping ratio is assumed for pile-soil system irrespective of mode of vibration.
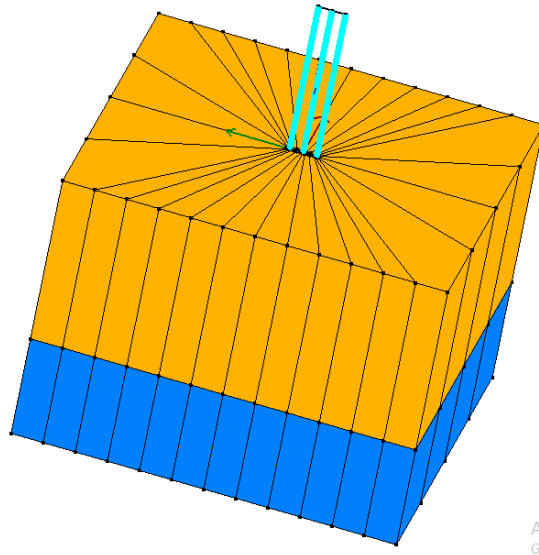
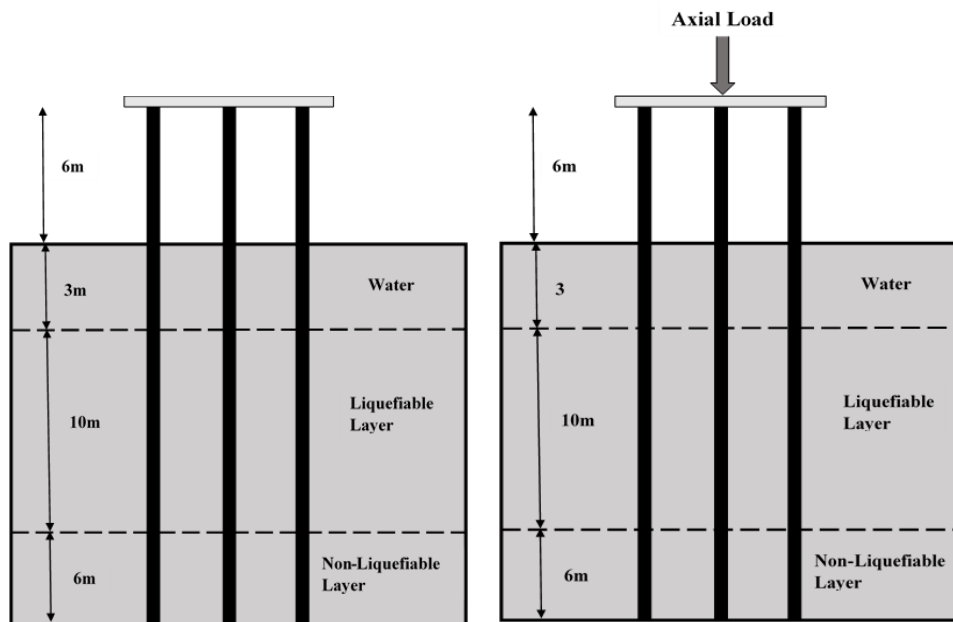*Figure 2*. Numerical model of soil-piled structure system modeled in OPENSeesPL 2.7.2

Figure 3. Schematic idealization of model of Showa Bridge pile and soil profile (a) without axial load and (b) with axial load.
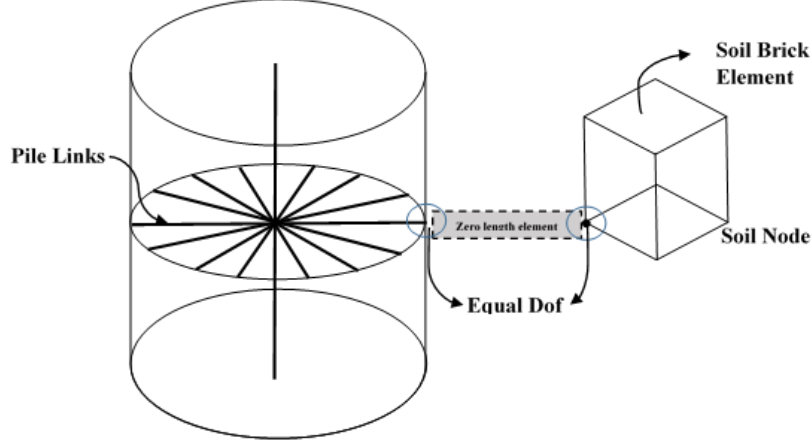
Figure 4. Soil and pile interaction through rigid links and zero length element

3   SELECTION OF GROUND MOTION

Selection of ground motion on the basis of variability of peak ground acceleration is a crucial task in strong motion seismology. Hence, it is important to quantify these variations correctly in seismic design process to ensure adequate safety and reliability of structures. Variability in source dimension, depth, epicentral distance etc. is to be considered for modeling of artificial ground motions [17]. Present study models such variability of ground motion using a simplified technique suggested by Haldar (2009 [11] which considered variability in acceleration based response spectral ordinates for generation of artificial ground motion. Haldar (2009) [11] presented that the variability associated with elastic response spectrum ordinates could be divided into three main classes as seismic source and attenuation variability (σ_{SE}), variability related to local geology and site condition (σ_{GS}) and variability associated with seismic force determination (σ_{RS}). Bea (1999) [12] suggested the value of σ_{SE} in respect of peak ground acceleration divided by gravitational constant for different seismo-tectonic characteristics of a location. The value of σ_{SE} in this study is assumed as 0.001g. The variability due to σ_{GS} is taken as 0.004g considering category of soil as class A [27]. The variability due to σ_{RS} is assumed as 0.003g considering variability in modeling uncertainty. These three categories of variability are combined to determine the resultant variability (σ_R) of the response spectrum ordinate, which is further utilized to determine the variability in the ground motion. The resultant variability (σ_R) is presented as follows,

$$\sigma_R = \sqrt{\sigma_{SE}^2 + \sigma_{GS}^2 + \sigma_{RS}^2} \qquad (1)$$

In present study, the ordinates of response spectrum are taken as log-normally distributed random variables for the analysis. The assumption of lognormal

distribution is valid because of non-negativity of the response spectrum ordinate and it has simple relation to normal distribution. Present study considers Indian Standard (IS) spectra for soft soil as mean spectra considering 5% damping and COV of spectral acceleration as 5% suggested as per Haldar (2009) [11].

Figure 5 presents randomly generated 30 realizations of response spectrum curve considering IS 1893-Part 1-2016 spectra as mean curve. The spectrum consistent artificial ground motions are generated using commercial program SeismoArtif 2018 [40]. The magnitude, hypocentral distance and similar soil condition of 1964 Niigata earthquake are selected as input parameters while generating the synthetic motions in SeismoArtif. For each spectrum curve, a set of eight artificial motions are generated and finally a total of 240 numbers of randomly generated ground motions are obtained for the analysis. A schematic representation of flowchart of generation of artificial motions in SeismoArtif (2018) is presented in Figure 6. Further, average time history signals (one representing lower bound of PGA and another one representing higher PGA) out of 30 sets of ground motions are presented in Figure 7.
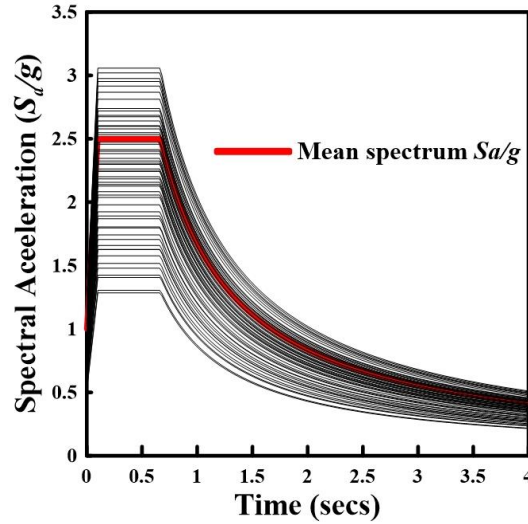

Figure 5. Randomly generated response spectra using MCS following IS 1893-Part 1-2016

Table 2. Ground motion characteristics

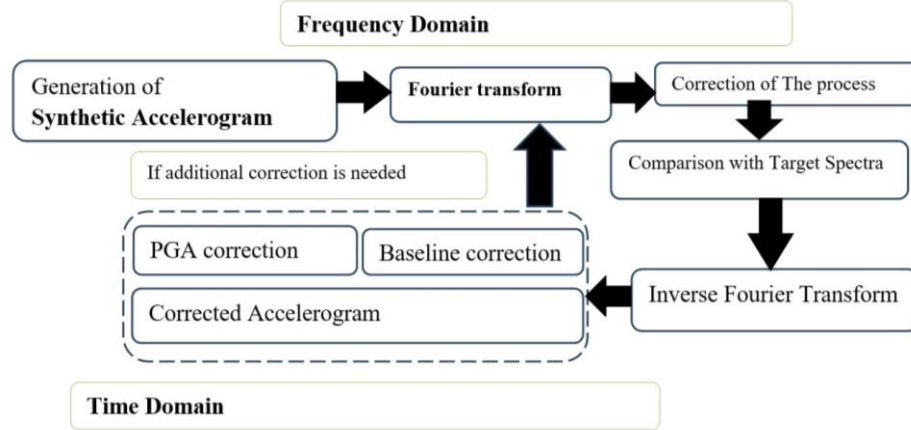| Parameters	Values
Regimes	Inter-plate regimes (Near Field)
Moment Magnitude (M_w)	7.6
Hypo central distance from station to event (km)	12
Soil Type	Generic soil
Shear wave velocity (V_s) (m/s)	320
Duration (secs)	32
Spectrum Factor	1.0

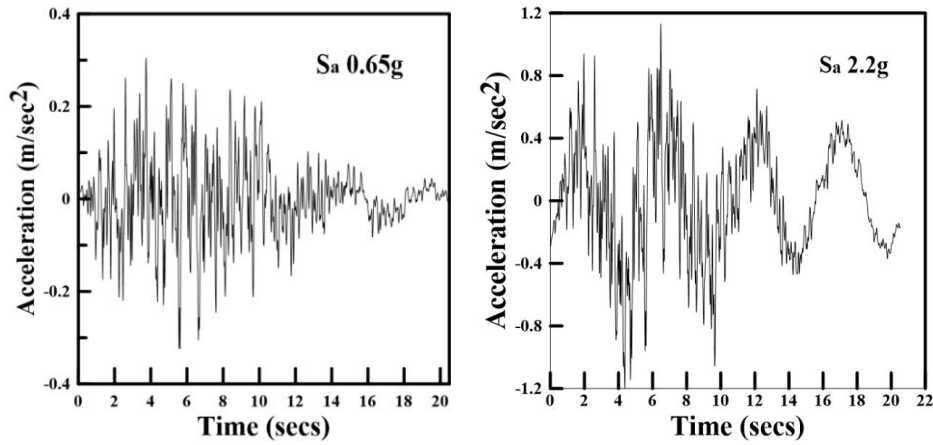*Figure 6.* Schematic chart of generation of synthetic ground motion

Figure 7. Acceleration time histories of artificially generated spectrum consistent ground motions.

4   DYNAMIC ANALYSIS

Nonlinear dynamic analyses were performed on 3D finite element model of soil-pile group system in OPENSeesPL. The incremental iterative procedure proposed by *Newmark's β-γ* time stepping method with time integration parameters $γ=6$ and $β=0.3025$ was used to integrate equation of motion. Krylov-Newton algorithm is considered to carry out the analyses for large number of DOFs. Initial tangent stiffness of the system is set for all the analyses and near about 40-50 iterations for every case are needed to achieve convergence tolerance (displacement increment) of 10^{-6}. Therefore, a total of 960 numbers of dynamic analyses considering all the four vertical loading conditions are carried out.

5   FRAGILITY ANALYSIS

5.1   Definition of limit state

In the present study, three different types of limit state parameter for pile foundation are defined. The maximum lateral displacement of 30 mm is considered for serviceability criteria limit state of pile foundation as per [13] and ultimate moment carrying capacity (M_u) i.e. the yield capacity 1280 kN-m is considered for collapse criteria limit state considering the diameter of the pile. Another limit state criterion is set in terms of curvature ductility demand of pile foundation as per [14]. According to HAZUS 97 [41], the limit states for curvature ductility demand (μ_ϕ) can be divided into four categories - slight, moderate, extensive and collapse state based on the amount of damage to pile foundation. The details of this limit state criterion and corresponding damage states of pile foundation are presented in Table 3. The ductility demand of pile foundation calculation is based on the equation suggested by [25].

Table 3. Curvature ductility demand (μ_φ) of pile foundation limit state parameters according to Hazus 97 (1999) [42]

	Damage parameter	Slight damage	Moderate damage	Extensive damage	Collapse damage
Limit state parameter	Curvature ductility demand (μ_ϕ) of pile foundation	$\mu_\phi > 1$	$\mu_\phi > 2$	$\mu_\phi > 4$	$\mu_\phi > 7$

5.2   Analysis procedure and vulnerability derivation

Fragility analysis is one of the many ways of expressing vulnerability of a system. Moreover, there are a number of procedures available to construct fragility curves. The fragility curves represent relationships between yielding the probability of reaching or exceeding a certain level of damage under excitation of certain intensity. Multiple strip analysis (MSA) method suggested by [15] is adopted in the present study to calculate seismic fragility of pile foundation. This method is one of the most common and reliable approach when using the conditional spectrum because the target properties of the ground motions change at each intensity measure (IM) level. Therefore, advantage with this approach lies in the fact that analyses need not to be performed up to IM amplitudes where all ground motions cause collapse. Maximum likelihood estimation is used for calculating mean (μ) and log standard deviation (σ) of fragility function for fitting of fragility curves [19]. The log of the likelihood function is maximized for determining μ and σ as presented in equation 2 following [15].

$$\{\hat{\mu}, \hat{\sigma}\} = \max \sum_{i=1}^{m} \{\ln\binom{n_i}{z_i} + z_i \ln \Phi(\frac{\ln x_i - \mu}{\sigma}) + (n_i - j_i)\ln(1 - \Phi(\frac{\ln x_i - \mu}{\sigma}))\} \qquad (2)$$

where x represents ground motion with $S_a=x,$ $\Phi()$ is normal cumulative distribution function, z represents total collapses, n represents number of ground motions, μ and σ represents mean and standard deviation of fragility function.

   In this study, the numerical model is analyzed considering total 240 numbers of spectrum consistent ground motions. The results of dynamic analyses are used for deriving fragility curves according to limit states. For each intensity level, number of failures out of eight analysis cases is represented as the probability of failure for that level. Therefore, the probability of failure increases with the increase in intensity level.

6   RESULTS AND DISCUSSION
6.1 Validation of numerical model
The accuracy and correctness of the FE model developed in OPENSeesPL [42] has been attempted to be validated against maximum ground displacement reported at Showa bridge site during 1964 Niigata earthquake. The seismic response of 3D FE model of ground is obtained considering N-S component of Niigata motion. Figure 8 presents the acceleration history of N-S component of Niigata motion. The maximum ground displacement is calculated as 20 cm as shown in Figure 9. As per [2], the maximum soil displacement at the recording site in the direction of bridge (30º North-West) was recorded about 22cm. So, the result from FEM developed indicates well agreement with the results obtained as per [2].
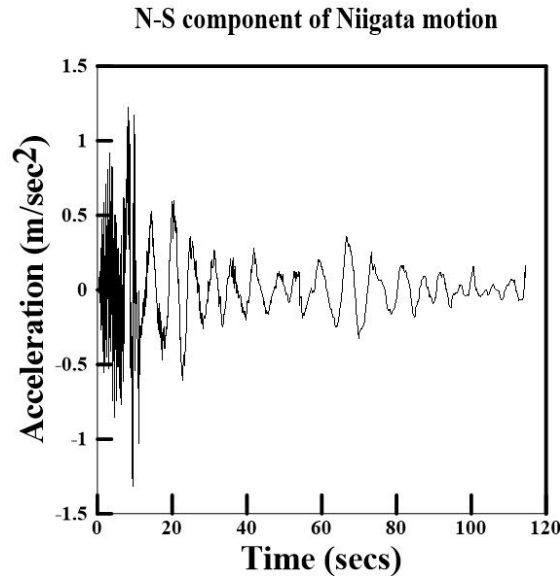

Figure 8. Recorded earthquake data of Niigata motion according to Bhattacharya et al. 2014 [2]
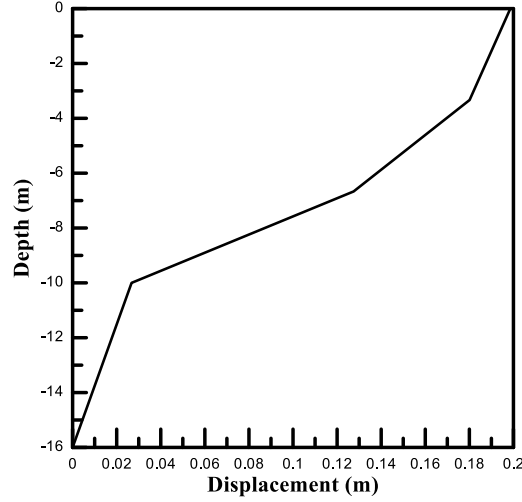
Figure 9. Maximum soil displacement profile of single pile numerical model for Niigata N-S component

6.2 Probabilistic seismic response of pile foundation

The responses of the numerical model of case study bridge structure are recorded from the dynamic analyses performed considering both inertial and kinematic interaction. The bending moment (M_{pile}) and displacement (δ_{pile}) at pile are recorded for different sets of ground motion along the depth of pile foundation which are presented in Figure 10 and 11 respectively. It can be observed from Figure 10 (a) and (b) that maximum bending moments are observed at a depth of about 10m from ground level for all the spectrum consistent ground motions irrespective of kinematic and inertial interaction respectively. The bending moments are found to vary within a range of 179 to 2785 kN-m in case of inertial interaction and 70 to 2290 kN-m in case of kinematic interaction for variation of S_a from 0.1g to 1.92g respectively. It is also observed that bending moment is marginally higher in case of inertial interaction compared to kinematic responses. This may be due to the initiation of P-Δ effect during inertial interaction. Further, it may also be noted that M_{pile} exceeds the ultimate moment capacity at $S_a = 1.12$g and 0.80g at a depth of 10m from ground level in case of kinematic and inertial interaction respectively. Similarly, pile head displacement also increases with increase in the intensity of base input excitation maximum. The maximum pile head displacement varies from 6.2 mm to 100 mm in case of inertial interaction and 5.8 mm to 86 mm in case of kinematic interaction respectively for variation of S_a from 0.1g to 1.92g at 8m above the ground surface i.e. at pile head. It is observed that δ_{pile} exceeds the permissible limit of 30 mm at S_a 0.71g and 0.65g for kinematic and

inertial interaction respectively. It is also observed that δ_{pile} exceeds serviceability criteria at a lesser PGA in comparison to collapse limit state criteria. This indicates serviceability criteria to be governing vulnerability check in case of pile supported in liquefiable soil.
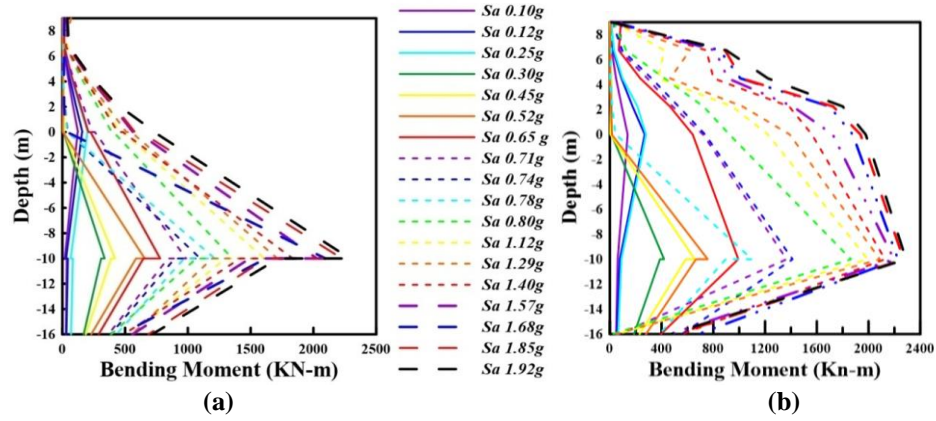

Figure 10. Variation of Bending Moment of piles for different Spectral acceleration (S_a) level for (a) kinematic interaction (b) inertial interaction.
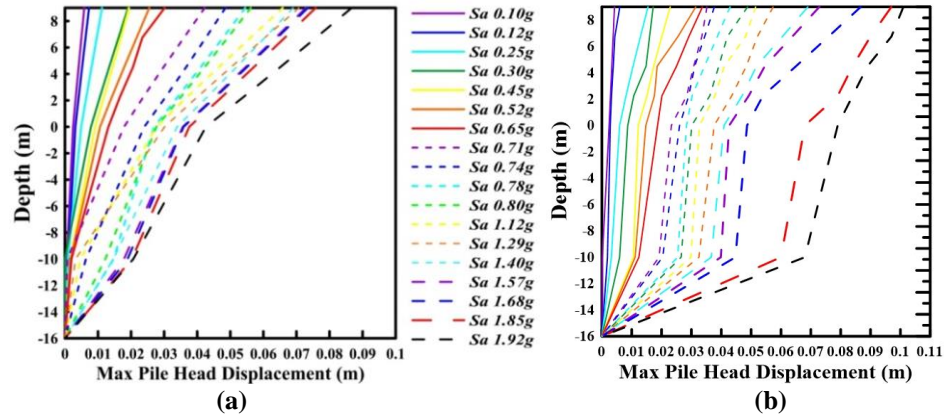

Figure 11. Variation of Maximum pile head displacement for different spectral acceleration (S_a) level for (a) kinematic interaction (b) inertial interaction.

6.3 Fragility curves

Fragility curves are developed for four cases of vertical loading i.e. 0%, 33%, 66% and100% of the total vertical load. Both serviceability as well as collapse limits state criteria are considered in order to derive the fragility curves. Figure 12 (a) and (b) presents fragility curves of serviceability and collapse limit state criteria respectively for 0% of vertical loading. Similarly, 13(a) and (b) presents

fragility curves of both the limit state criteria for 33%, 66% and 100% of vertical loading. The fragility curves are derived based on responses of pile foundation recorded from the dynamic analyses. It can be observed from Figure 12(a) that 50% probability of failure (POF) is exceeded at PGA of 0.18g for serviceability limit state criteria considering 0% of vertical loading. Whereas in case of collapse limit state criteria, the same POF is found to exceed at PGA of 0.36g as observed from Figure 12(b). The PGA of earthquake motion in case of collapse limit state is found to be around two times higher compared to serviceability limit state condition at POF = 50%. This infers that serviceability criteria seem to be the governing factor in seismic design of pile foundation embedded in liquefied deposit. Similar trend is observed for 33%, 67% and 100% of axial loading cases as presented in Figures 13 (a) and (b).
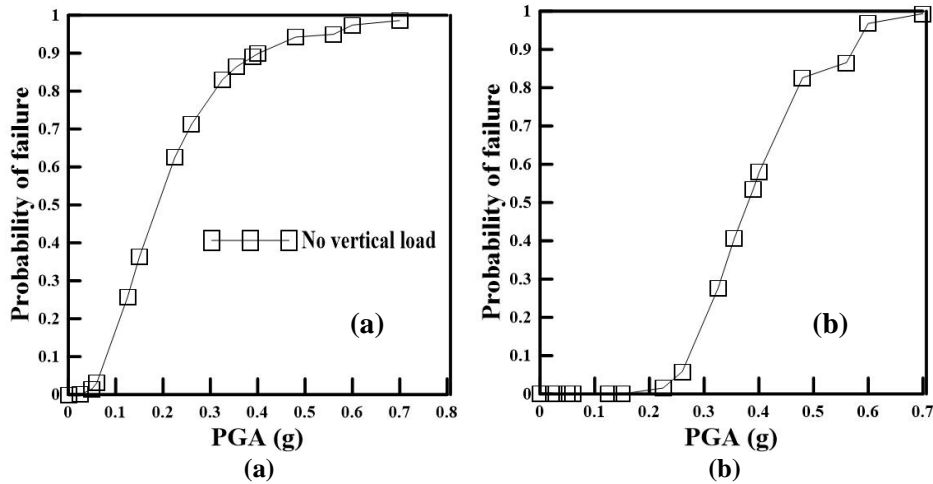

Figure 12. Fragility curves for zero load condition (a) serviceability state and (b) collapse limit state criteria

Considering curvature ductility demand (μ_ϕ) limit state of pile, the fragility curves are developed for 0% and 100% vertical loading as presented in Figure 14 (a) and (b) respectively. The curvature ductility demand (μ_ϕ) are calculated from the maximum bending moment recorded at pile head under the influence of different sets of ground motion. For 0% of vertical loading and 50% POF, slight, moderate, extensive and collapse damage are observed at PGA of 0.02g, 0.08g, 0.11g and 0.22g respectively as observed in Figure 14(a). Similarly, for 100% of vertical loading, 50% POF is exceeded at PGA of 0.01g, 0.015g, 0.03g and 0.05g for the four damage states as observed in Figure 14(b). Therefore, it is observed that POF with respect to curvature ductility demand of pile exceeds at relatively lower PGA irrespective of damage states in case of 100% vertical

loading that to 0% vertical loading. Further, Table 4 presents comparison of intensity measure of ground motions at POF=50% considering serviceability, collapse and curvature ductility demand limit state criteria. It is found that μ_ϕ seems to be governing design criteria for pile foundation in liquefied soil as compared to conventional other design criteria.
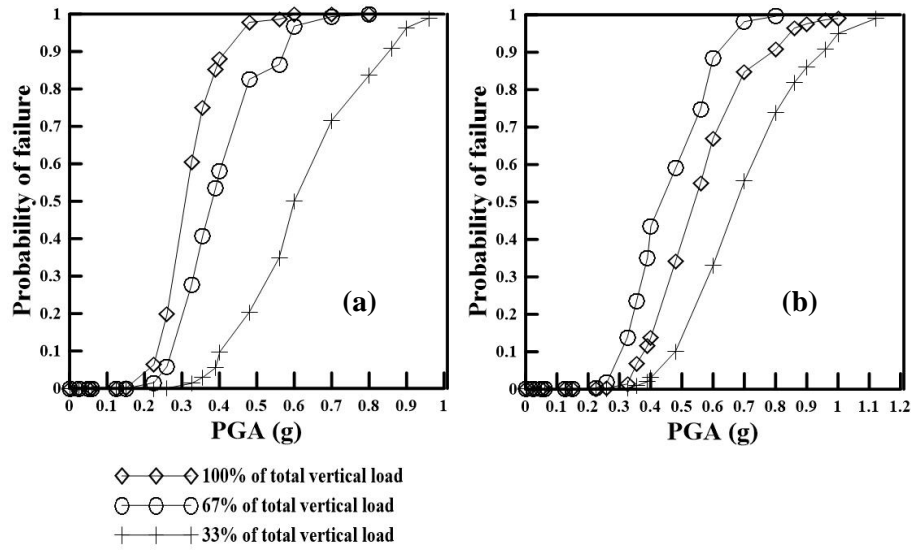

Figure 13. Fragility curves for kinematic interaction (a) serviceability state and (b) collapse limit state criteria.
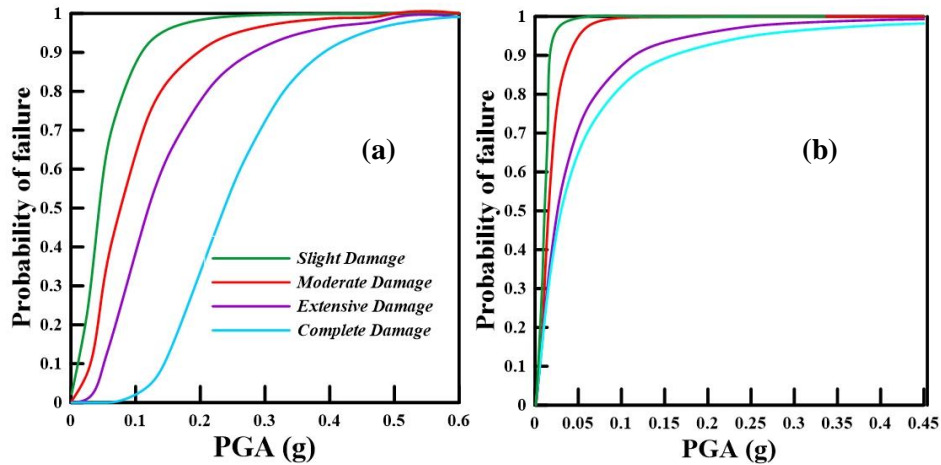

Figure 14. Fragility curves for pile foundation in terms of ductility demand for (a) 0% axial load and (b) 100% axial loading.

It is further to be noted that the PGA of 1964 Niigata motion was 1.2g which caused failure in pile foundation of Showa Bridge. However, fragility analysis performed in present study indicates that POF of 90% is achieved at PGA of 1.0g in case of inertial interaction (100% vertical load). This infers the sanctity of vulnerability analysis incorporating SSPSI in present study. Besides, study also highlights that POF of 90% is also found at a lesser PGA of 0.55g when kinematic interaction (0% of vertical load) was considered.

Table 4. Comparison of intensity measure of ground motions at POF=50% considering serviceability, collapse and curvature ductility demand limit state criteria

Target Probability of failure (POF)	Vertical loading cases	Intensity measure (PGA) (g) at different limit states					
		Serviceability	Collapse	Curvature ductility demand damage states			
				Slight	Moderate	Extensive	Collapse
50%	0%	0.18	0.37	0.02	0.08	0.11	0.22
	33%	0.28	0.42	-	-	-	-
	67%	0.36	0.51	-	-	-	-
	100%	0.58	0.70	0.01	0.015	0.03	0.05

7   SUMMARY AND CONCLUSIONS

Present study highlights the vulnerability of pile foundation embedded in liquefiable susceptible ground by constructing fragility curves. The case study of Showa bridge failed during 1964 Niigata earthquake is considered herein for analysis. Both kinematic and inertial interaction failure mechanism are considered to develop the fragility curves. Bending moment of pile foundation (M_{pile}) and pile displacement (δ_{pile}) are recorded from the dynamic analyses performed. The numerical model developed in present study using OPENSeesPL (*V*-2.7.2, 2018) [42] is validated with physical observations of Showa bridge site after 1964 Niigata earthquake which indicates a well agreement with the results obtained from present study. Finally, the study leads to following broad conclusions.

1. Maximum bending moment at pile irrespective of intensity of ground motions (S_a) is observed at the interface of liquefiable and non-liquefiable layers i.e. at a depth of 10m below ground surface. While such responses are higher in case of inertial interaction compared to kinematic interaction. This may be due to P-Δ effect during inertial interaction. On the other hand, pile displacement also increases with increase in S_a; and reaches maximum at

above 8m from ground level irrespective of all ground motions. The maximum displacement at pile head is also slightly higher in inertial case compared to kinematic interaction.

2. Fragility curves are developed for both serviceability and collapse criteria attributing 0%, 33%, 67% and 100% of total axial load. Results indicate that probability of failure (POF) is higher pertaining to serviceability limit state as compared to collapse criteria. For instance, 90% POF attained at PGA of 0.45g and 0.58g considering serviceability and collapse criteria respectively in case of zero percentage of axial loading (i.e. kinematic interaction). Similar trend is observed irrespective of all other loading cases. Therefore, serviceability limit state seems to be governing criteria in design of pile foundation.

3. Fragility curve for pile foundation developed based on curvature ductility limit state indicates that POF is significantly increased in case of slight damage state as compared to other damage states irrespective of loading cases. Comparing the fragility curves for 0% and 100% axial loading condition, it is also observed that for inertial interaction (100% of axial load) POF is relatively higher as compared to kinematic interaction. Further, it can be observed from comparison of fragility curves considering all the limit states that curvature ductility demand is the governing limit state criteria for design of pile foundation embedded in liquefied soil.

Therefore, present study offers an insight into the vulnerability of pile foundation embedded in liquefiable deposit highlighting a case study of pile failure due to liquefaction. Fragility analysis performed considering both kinematic and inertial interaction validates reasonably well with the reported failure of the Showa bridge. Moreover, it may be concluded that curvature ductility demand is a governing limit state criteria for reliability based seismic design of pile foundation. However, this issue needs to be validated by another study considering parametric variation of bridges and other probabilistic methods.

REFERENCES

1. Meymand, P. J (1998). "Shaking table scale model tests of nonlinear soil-pile-superstructure interaction in soft clay". (Doctoral dissertation, University of California, Berkeley)
2. Bhattacharya, S. Tokimatsu, K.Goda, K.Sarkar, R.Shadlou, M. Rouholamin, M. 2014. "Collapse of Showa Bridge during 1964 Niigata earthquake: A quantitative reappraisal on the failure mechanisms", *Soil Dynamics and Earthquake Engineering*, 65 (2014) 55–71.
3. Bhattacharya S, Dash SR, Adhikari S. "On the mechanics of failure of pile-supported structures in liquefiable deposits during earthquakes". CurrSci 2008b;94(5):605–11.
4. Bhattacharya S, Tokimatsu K. "Collapse of Showa Bridge revisited" .Int J Geoeng Case Hist 2013; 3(1):24–35.
5. Hamada M, O'Rourke TD. "Case studies of liquefaction and lifeline performance during past earthquakes. Japanese case studies", Technical Report NCEER-92- 0001; 1992.
6. Kumar C.M.R, Narayan K.S.B, Reddy D. Venkat (2014). "Methodology for Probabilistic

     Seismic Risk Evaluation of Building Structure Based on Pushover Analysis." *Open Journal of Architectural Design*, 2(2):13-20.

7. Tokimatsu K, Suzuki H, Sato M. "Effects of Inertial and kinematic interaction on seiasmic behavior of pile with embedded foundation". *Soil Dynamics and Earthquake Engineering* 2005;25(?):753–62.

8. Kwon, O.S. Elnashai, A. "The effect of material and ground motion uncertainty on the seismic Vulnerability curves of RC structure", Engineering Structures, 28 (2006) 289–303.

9. Zhang, J. Huo, Y. Brandenberg, S.J. Kashighandi, P. 2008. "Fragility Functions of Different Bridge Types Subject to Seismic Shaking and Lateral Spreading". The 14th World Conference on Earthquake Engineering, Beijing, China.

10. Zentner I, Gündel M, Bonfils N (2016). "Fragility analysis methods: Review of existing approaches and application" *Nuclear Engineering and Design*.

11. Haldar, S. Babu, G.L.S, "Probabilistic Seismic Design of Pile Foundations in Non-Liquefiable Soil byResponse Spectrum Approach", *Journal of Earthquake Engineering*, 13:737–757, 2009.

12. Bea, R.G. 1999. "Reliability based Earthquake design guidelines for marine structures", *Journal of Waterway, Port, Coastal and Ocean Engineering*, ASCE, Vol.125 (5),219-231.

13. Das, B. Saha, R. Haldar, S. 2016. "Effect of in-situ variability of soil on seismic design of piled raft supported structure incorporating dynamic soil-structure-interaction", *Soil Dynamics and Earthquake Engineering* ,84(2016)251–268.

14. Choi, E. DesRoches, R. Nielson, B. 2003. "Seismic fragility of typical bridges in moderate seismic zones", *Engineering Structures* 26 (2004) 187–199.

15. Baker J.W, M. EERI (2011). "Efficient analytical fragility function fitting using dynamic structural analysis." *Earthquake Engineering & Structural Dynamics*, 34(10), 1193–1217.

16. Kramer SL. Geotechnical earthquake engineering. Civil Engineering and Engineering Mechanics Series. Prentice-Hall; 1996.

17. Sigbjörnsson R. 2004. "Uncertainty analysis of strong ground motion". 13th World Conference on Earthquake Engineering Vancouver, B.C., Canada, Paper No. 1536.

18. Velez, A., Gazetas, G. and Krishnan, R. (1984), "Lateral dynamic response of constrained head piles", *Journal of Geotechnical Engineering*, ASCE, v. 109(8), pp. 1063-1081.

19. Masanobu Shinozuka; M. Q. Feng; Jongheon Lee; and Toshihiko Naganuma (2000) "Statistical Analysis of Fragility Curves", *Journal of Engineering Mechanics, ASCE,* v.126 (12).

20. Chan CL, Low BK. (2012), "Probabilistic analysis of laterally loaded piles using response surface and neural network approaches," *Computer and Geotechnics*, 43:101–10.

21. Chanda D., Saha R. and Haldar S. (2019), "Influence of inherent soil variability on seismic response of structure supported on pile foundation", *Arabian Journal for Science and Engineering,* 44:5009–5025.

22. Matlock H. (1970), "Correlations for Design of Laterally Loaded Piles in Soft Clay", *Proceedings of 2nd Annual Offshore Technology Conference*, Houston, pp. 577-594.

23. Mylonakis G, Syngros C, Gazetas G and Tazoh T. (2006), "The role of soil in the collapse of 18 piers of Hanshin Expressway in the Kobe earthquake", *Earthquake Engineering and Structural Dynamics,* 35:547–575.

24. Pula W. and Rozanski A. (2012), "Reliability of rigid piles subjected to lateral loads," *Archives of Civil and Mechanical Engineering*, 12(2):205-218.

25. Song S. T., Chai Y. H. and Hale T.H. (2004), "Limit state analysis of fixed-head concrete piles under lateral loads", 13th*World Conference on Earthquake Engineering,* Vancouver, B.C., Canada.

26. Tandjiria V, Teh CI, Low BK. (2000), "Reliability analysis of laterally loaded piles using response surface methods", Structal Safety, 22:335–55.

27. IS: 1893 Part 1 (2016), *Indian Standard Code of Criteria for Earthquake Resistant Design of Structures*, Bureau of Indian Standards New Delhi India.

28. Boulanger R.W., Curras C.J., Kutter B.L., Wilson W.D. and Abghari A.A. (1999), "Seismic soil–pile– structure interaction experiment sand analyses", *Journal of Geotechnical Geoenvironmental Engineering, ASCE*, 125(9):750–9.

29. Ghosh, B.; Lubkowski, Z. (2007), Modeling dynamic soil structure interaction under seismic loads. In: S. Bhattacharjee (ed.) Design of Foundations in Seismic Areas: Principles and Applications, pp.118–198. IIT Kanpur, NICEE, India.

30. Kaynia MA, Mahzoon PS. Forces in pile foundations under seismic loading. J Eng Mech1 996; 122(1):46–53.

31. Badoni, D. and Makris, M. 1996. Nonlinear response of single piles under lateral inertial and seismic loads. Soil Dynamics and Earthquake Engineering, 15: 29-43.

32. Baranov, V. A. 1967. On the Calculation of Excited Vibrations of an Embedded Foundation (in Russian), Voprosy Dinamiki i Prochmosti, No. 14, Polytechnic Institute Riga, 195-209.

33. Guin, J. and Banerjee P. K. 1998. Coupled Soil-pile-structure Interaction Analysis Under Seismic Excitation. Journal of Structural Engineering, ASCE, 124(4): 434-444.

34. Kuhlemeyer, R. L. 1979. Static and Dynamic laterally loaded piles. Journal of the Geotechnical Engineering Division, ASCE, 105, GT2, 289-304.

35. Maheswari, B. K, Truman, K. Z., Gould, P. L. and Naggar, E. M. H. 2005. Three-dimensional Nonlinear Seismic analysis of Single piles using Finite element Model: Effects of plasticity of soil, International Journal of Geo-mechanics, ASCE, 5(1): 35-44.

36. Kagawa, T. and Kraft, M. L. 1980. Lateral Load-Deflection relationships of piles subjected to dynamic loadings, Soils and Foundation, JSSM&FE, 20(4): 19-36.

37. Naggar E. MH. and Novak M. 1996. Nonlinear Analysis for Dynamic Lateral Pile Response. Soil Dynamics and Earthquake Engineering, 15: 233-244.

38. Nogami T., Otani J. and Chen, H. 1992. Nonlinear Soil-Pile Interaction Model for Dynamic Lateral Motion. Journal Geotechnical Engineering, ASCE, 118(1): 89-106.

39. Yang Z, Lu J, Elgamal A (2008). OpenSees soil models and solid-fluid fully coupled elements. User's Manual, Version 1.0.

40. SeismoArtiff (2016). Earthquake Software for Artificial Accelerograms Generation, Available from URL: http://www.seismosoft.com.

41. HAZUS (1999). Earthquake Loss Estimation Methodology HAZUS™ User's Manual. SR2 Edition. National Institute of Building Sciences for Federal Emergency Management Agency, Washington, D.C.

42. OPENSeesPL V-2.7.2 (2018). 3D Lateral Pile-Ground Interaction, Available from URL: http://soilquake.net/openseespl/